

Design and Performance Analysis of Defected Ground Slotted Patch Antenna for Sub-6 GHz 5G Applications

Md. Najmul Hossain^{1,*}, Al Amin Islam¹, Md. Abdur Rahim², Md. Imran Hossain³, and Md Arifour Rahman⁴

¹Department of Electrical, Electronic and Communication Engineering, Pabna University of Science and Technology, Pabna-6600, Bangladesh

²Department of Computer Science and Engineering, Pabna University of Science and Technology, Pabna-6600, Bangladesh

³Department of Information and Communication Engineering, Pabna University of Science and Technology, Pabna-6600, Bangladesh

⁴Department of Electrical and Electronic Engineering, University of Rajshahi, Rajshahi-6205, Bangladesh

Received: November 04, 2023, Revised: December 25, 2023, Accepted: December 25, 2023, Available Online: December 31, 2023

ABSTRACT

Recently, there have been notable advancements in wireless communication systems to address the deficiencies of fourth generation (4G) wireless technology, such as insufficient spectrum bandwidth, slow data transfer rates, and constrained network capacity. These issues may be addressed in fifth generation (5G) wireless technology, which is no longer stand-alone. This article proposes and designs a defected ground slotted patch antenna (DGSPA) for 5G (Sub-6 GHz band) applications. It can work at 3.5 GHz in the 5G N77 band, Sub-6 GHz 5G, LTE Band 42, and WiMAX. The suggested antenna has an overall dimension of $38 \times 38 \times 1.575$ mm³ and is built on the Rogers RT5880 substrate material, whose dielectric permittivity is 2.2. The CST software is used as the simulation tool to analyze the designed antenna's performance. The novelty of the recommended antenna is in terms of its small size with defective ground structure (DGS), high antenna gain, perfect impedance matching, and improved impedance bandwidth. The role of the DGS is evaluated by comparing the antenna's performance with and without the DGS. It has been noticed that the DGS-backed antenna had an impedance bandwidth improvement of more than 11MHz, whereas the impedance profile is $(50.086 - j0.179) \Omega$, which denotes 50Ω pure resistivity. It will operate within the frequency range of (3.4828 - 3.522) GHz with an impedance bandwidth of 69.2 MHz. The proposed antenna's reflection coefficient ($|S_{1,1}|$) is obtained as -54.028 dB at the resonating frequency of 3.5176 GHz, whereas the radiation gain and efficiency are observed as 6.463 dB and 93.475%, respectively. Thus, due to its promising performance based on radiation pattern, optimum efficiency, and higher bandwidth, the recommended defected ground slotted patch antenna can efficiently be used for the application of Sub-6 GHz 5G services.

Keywords: Slotted Patch Antenna, DGS, High Gain, Sub-6 GHz Band, 5G Applications



Copyright @ All authors

This work is licensed under a [Creative Commons Attribution-Non Commercial 4.0 International License](https://creativecommons.org/licenses/by-nc/4.0/).

1 Introduction

Wireless communication networks (WCNs) have entered a new era by introducing 5G technology. It offers several benefits over multipath environments, such as faster data rates, massive connection, low latency, wide coverage area, and many more. 5G technology is now essential in many sectors of human life, including communication, commerce, education, and transportation [1], [2]. Due to smart devices being defined as mobile users on the Internet of Things (IoT), 4G technology is insufficient to meet the increasing demand for data. In users' eyes, the key difference between 4G and 5G technology is enhanced data rate and lower power consumption with huge coverage. Cellular communication is now commonly employed in the Sub-6 GHz band, mostly at frequencies below 3 GHz. The frequency spectrum of 5G networks is divided into two ranges: Sub-6 GHz band and above-6 GHz band [3], [4].

Compared to today's 4G LTE networks, 5G uses several significant new technology advancements to significantly increase the spectrum used for data transmission and reception. For consumers, these technologies enable substantially higher speeds and more capacity [5], [6]. Following are the few technologies that are compatible with the 5G connectivity:

Sub-6 GHz: Most forthcoming 5G networks are expected to function predominantly inside the mid-band frequencies, ranging from 3 to 6 GHz, like WiFi. In addition to being helpful for more powerful outdoor base stations or small cell hubs for usage within, it covers the medium-range spectrum.

mmWave: To facilitate fast data transfer, it has a very high-frequency range of 17 to 110 GHz. It is a short-range technology that is intended for usage in crowded environments.

Beamforming: Beamforming is an important technology for addressing the limits in range and direction of the high-frequency waveform spectrum. By employing beamforming, wireless communications can be enhanced in terms of strength, speed, and reliability. It is achieved by directing signals towards consumer devices.

Massive MIMO: Utilizing multiple antennas on base stations, data is transferred and received to facilitate many users. The high-frequency networks are now significantly more effective due to this technology. Additionally, beamforming may be coupled with it.

A growing standard, 5G combines more spectrums and offers more bandwidth. Fig. 1 shows the networking spectrum bands, whereas carriers also utilize existing 4G LTE channels, low bands below 1 GHz, and new spectrum in the sub-6 GHz

WiFi region [6]. The C band (3.4–3.6 GHz) was suggested for 5G technology by following a thorough review of the 5G candidate frequency bands below 6 GHz in [7]-[11]. Recently, the most developed nations in the world, such as the United States, Canada, United Kingdom, Japan, China, Korea,

Australia, and several other countries, adopted the specifications of 5G communication technology standards. The global spectrum for Sub-6 GHz 5G systems is briefly described in Table 1 [12]-[16].

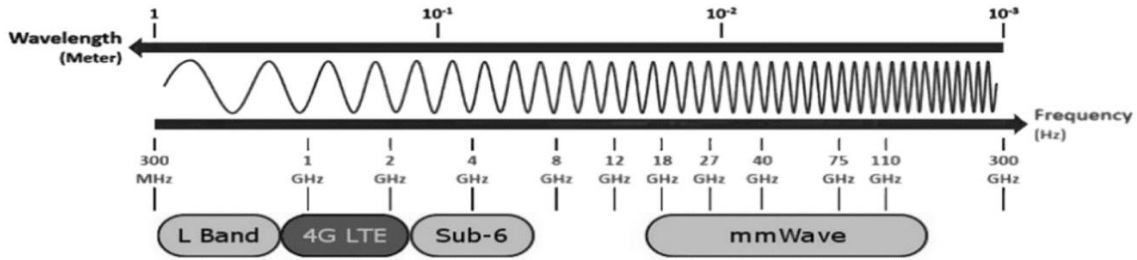


Fig. 1 Networking spectrum bands [6]

Table 1 Global Spectrum Details for Sub-6 GHz 5G [12]-[16]

Countries	(3– 4) GHz Band	(4–5) GHz Band	(5–7) GHz Band
China	(3.3 – 3.6) GHz	(4.5 – 5.0) GHz	--
UK	(3.4 – 3.8) GHz	--	--
USA	(3.45 – 3.7) GHz (3.7 – 3.98) GHz	(4.49 – 4.99) GHz	(5.9 – 7.1) GHz
Canada	(3.47 – 3.65) GHz (3.65 – 4.0) GHz	--	(5.9 – 7.1) GHz
Australia	(3.4 – 3.7) GHz	--	--
Italy	(3.6 – 3.8) GHz	--	--
India	(3.4 – 3.6) GHz	--	--
Malaysia	3.5 GHz	--	--
Korea	(3.4 – 3.7) GHz (3.7 – 4.0) GHz	--	--
Japan	(3.6 – 4.1) GHz	(4.5 – 4.9) GHz	--
EU	(3.4 – 3.8) GHz	--	(5.9 – 6.4) GHz

transmission at Sub-6 GHz is challenging. Patch antennas may be a good option for this type of network because of their many benefits, including low profile, affordable price, sustainable gain, ease of fabrication, etc. The signal is fed to the patch antenna through various feeding techniques, including microstrip line, proximity coupled, inset feed, aperture coupled, and coaxial probe feed [18].

In this manuscript, we propose a defected ground slotted patch antenna (DGSPA) using a coaxial feeding technique for 5G services in the Sub-6 GHz frequency band. The main objective of this research is to design a compact high gain 5G smart antenna that operates at Sub-6 GHz and meets the requirements for a variety of 5G wireless applications. The antenna without DGS will operate within the frequency range of (3.6106 - 3.6682) GHz, resonating at 3.6396 GHz with a return loss of -37.916 dB. In the presence of DGS, it resonates at 3.5176 GHz frequency with an excellent return loss of -54.028 dB and operates from 3.4828 GHz to 3.522 GHz frequency range. Due to DGS, the bandwidth of the recommended antenna is increased by 11.6 MHz, and the reflection coefficient is decreased by -16.112 dB. Its impedance profile is $(50.086 - j0.179) \Omega$, which denotes perfect impedance matching. Therefore, the proposed patch antenna is suitable for Sub-6 GHz 5G communication services.

2 Literature Review

Numerous research has been conducted and are still working on 5G antennas. Radiofrequency (RF) experts recently created

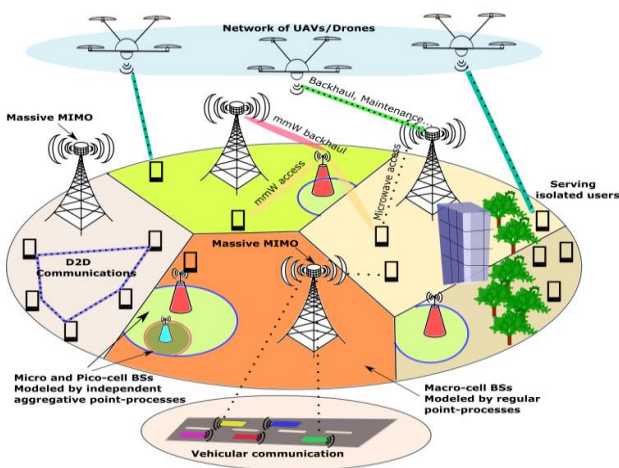


Fig. 2 The primary elements of a typical 5G network architecture [17]

Moreover, micro and macro cells are depicted in a general 5G network in Fig. 2, with the microcells represented by aggregative point processes [17]. An antenna is required for wireless communication systems to transmit and receive data using electromagnetic waves. The antenna serves as an interface between free space and a guiding device. 5G technology necessitates compact antennas with excellent performance. Designing high-performance, small-size antennas for 5G

multiple antennas for 5G sub-6 GHz communications using various methods, i.e., meta-material (MTM), complementary split-ring resonators (CSRR), slot formation, defective ground structure (DGS), artificial dielectric, and many more. The summary information from the research articles and a description of the relevant parameters are discussed below.

The authors of [19] suggested two different types of meta-material (MTM) antennas for 5G IDAS applications. Both antennas can operate at 3.5 GHz. The triangular and rectangular patches that comprise the antenna's radiating structure are combined with two etched complementary split-ring resonators (CSRR) unit cells on the top layer. Both antennas used FR4 material as substrate and have complete ground planes and 3×3 cross-slot MTM on the bottom layer. The measured gain characteristics of the two proposed MTM antennas are 2.6 dBi and 2.3 dBi, respectively, which are relatively low. Also, their structures are complicated, although both antennas are small. For 5G wireless applications, a bow-tie patch antenna with DGS is suggested in [20]. The antenna's impedance bandwidth was improved using a defective ground structure (DGS) built on an FR-4 substrate, and the measured impedance bandwidth was 13.37%. At 3.5 GHz, the simulated antenna gain was 8.38 dBi. It has a large volume of $90 \times 80 \times 1.6 \text{ mm}^3$, one of its key disadvantages. In [21], a meta-surface hybrid antenna is suggested. It has a huge dimension of $52.62 \times 40.40 \text{ mm}^2$ but offers excellent impedance bandwidth (185 MHz) and gain (6.74 dB).

The authors of [22] suggest a patch antenna with parasitic strips. It features a low profile and wider bandwidth but a poor gain (0.576 dBi) for 5G services operating at the Sub-7 GHz band. The authors of [23] propose a wideband Y-slot patch antenna with a felt substrate for medical and 5G applications. It combines a fabric-metal barrier operating at 2.4 GHz 65.4% with a low specific absorption rate and a gain of 6.48 dBi. But its overall dimension is relatively large. In [24], a unique miniature 5G antenna is presented using slots and metamaterial components. It has an excellent bandwidth of 774 MHz and a moderate gain of 3.44 dB. A high-gain patch antenna is designed and studied in [25] for mobile TV, radar, and other future wireless applications. It has a narrow band (23.6 MHz) and occupies a huge dimension of $100 \times 100 \times 1.6 \text{ mm}^3$.

The authors of [26] proposed a circular patch antenna based on a synthetic dielectric substrate for 5G communications in the Sub-6 GHz range. It has a very good bandwidth (196 MHz) and a 6.391 dB radiation gain at a 3.5 GHz resonant frequency. But its dimensions ($45 \times 40 \times 4.5 \text{ mm}^3$) are comparatively large. In [27], a dual-band slotted shape patch antenna with dimensions of $50 \times 30 \times 1.57 \text{ mm}^3$ for 5G services is presented. It was constructed on Rogers 5880 material. At the resonant frequencies, there is a radiation gain of 7.52 dBi and 5 dBi, respectively. But it offers both bands a narrow bandwidth. In [28], an array antenna based on a conductive graphene film is presented for 5G services with a 6.77 dBi radiation gain at the resonance frequency. Its volume ($60 \times 70 \times 1.6 \text{ mm}^3$) is relatively very large.

For 5G (C-Band) access point services, the authors of [29] present a high profile ($88.5 \times 88.5 \times 1.6 \text{ mm}^3$) 4-element array antenna, which has been developed on FR4 (Flame Retardant 4) dielectric material. Its radiation efficiency is very poor (approximately 30%), although it offers good impedance bandwidth. Utilizing three different dielectric materials, FR-4, RT-5880, and TLC-30, a rectangular-shaped patch antenna is

proposed in [30]. Design-2 offers a radiation gain of 4.660 at a 3.5 GHz resonant frequency. In [31], another patch antenna for 5G services is introduced utilizing four dielectric materials. The Arlon AD300C material performs the best and offers a radiation gain of 7.15 dBi at 5.65 GHz. But its overall dimension is relatively large. With dimensions of $47.46 \times 36.57 \times 1.5 \text{ mm}^3$, a rectangular shape patch antenna for 5G communication systems using rhombic slots is presented in [32]. It has a directivity of 6.158 dBi at a frequency of 3.5305 GHz. A novel metasurface-based patch antenna for Sub-band 5G communication is introduced in [33]. At 4.8 GHz frequency, it provides a high radiation gain and excellent bandwidth (7.68 dBi/220 MHz). But it features a very large volume of $75 \times 60 \times 15 \text{ mm}^3$.

A compact ($32 \times 25 \times 0.254 \text{ mm}^3$), flexible CPW-fed patch antenna is presented in [34] specially designed for 3.5 GHz 5G communication and 2.45 GHz ISM band. It has a wide impedance bandwidth (210/1300 MHz) but exhibits a poor radiation gain (1.74, 2.51 dB) in terms of both bands. In [35], a novel fractal geometry-based compact patch antenna for 5G wireless communications was introduced. Over the operational frequency range, it offers a radiation gain of more than 3 dBi and is built on Roger dielectric material. The authors of [36] introduced a letter-slotted dual-band patch antenna for a 5G Sub-6 GHz application. At frequencies of 4.53 GHz and 4.97 GHz, it provides radiation gains of 5 dB and 4.57 dB, respectively. It is printed on the RO5880 dielectric material with a huge dimension ($77 \times 70.11 \times 1.6 \text{ mm}^3$). Moreover, a frequency selective surface (FSS) reflector equipped with a high profile ($166 \times 66 \times 1.6 \text{ mm}^3$) microstrip antenna is proposed in [37] for use in 5G services. Its radiation gain at 4.1 GHz frequency is 12.4 dBi, and its fractional bandwidth is 51.12%.

For LTE/Sub-6 GHz 5G services, a multi-slotted low-profile patch antenna is recommended in [38], which operates from 3.15 to 5.55 GHz frequency. However, its maximum radiation gain in the operational band is only 2.69 dBi. A high-dimensional ($120 \times 60 \times 0.5 \text{ mm}^3$) planar multiband antenna is recommended for GSM, UMTS, LTE, and 5G wireless services [39]. It operates at 900 MHz, 2.4 GHz, 3.5 GHz, and 5.2 GHz. At 2.4 GHz, it exhibits a maximum radiation gain of 4.08 dB. In [40], an octa-band shared aperture square concentric slotted antenna with a size of $50 \times 50 \times 0.508 \text{ mm}^3$ is presented for mmWave band 5G applications. It has a minimum impedance bandwidth of 180 MHz and exhibits a 10.2 dB gain at 28 GHz. The authors of [41] recommend a novel planar slot antenna with parasitic elements and DGS, which can work on LTE Band 42, WiMAX, and 5G networks. It is relatively small and offers a good radiation gain. However, its bandwidth is very limited (only 19 MHz).

3 Design Methodology of the Defected Ground Slotted Patch Antenna

In wireless communication, patch antennas are most typically used to transmit electromagnetic (EM) waves into space. A microstrip patch antenna mainly comprises three basic parts: patch, dielectric substrate, and ground plane. Microstrip antennas are commonly known as patch antennas. The radiating elements and feed lines are typically fabricated by the process of photoetching on the dielectric substrate. Microstrip antennas can be designed using a variety of substrates, both thick and thin. A thick dielectric substrate provides enhanced efficiency, wider bandwidth, and loosely confined fields for radiation into space.

Conversely, a thin dielectric substrate allows for reduced dimensions of the elements. The function of the ground plane between the substrates is to isolate the feed from the radiating element and minimize interference of spurious radiation for pattern formation and polarization purity [42]. It has a ground plane on one side and a dielectric substrate material on the other and can be square, elliptical, circular, rectangular, or even a ring in shape.

3.1 Background

The following equations can be used to determine the length L and width W of any rectangular patch antenna [20], [22].

$$W = \frac{c}{2f_0\sqrt{\frac{\epsilon_r + 1}{2}}} \quad (1)$$

where ϵ_r denotes the dielectric constant and f_0 is the resonance frequency. The radiation propagates through the atmosphere and partially penetrates the substrate to reach the ground. Because the dielectric constants of the air and the substrate are different from each other, it is necessary to consider an effective dielectric constant (ϵ_{eff}), which is determined using the provided equation [22].

$$\epsilon_{eff} = \frac{\epsilon_r + 1}{2} + \frac{\epsilon_r - 1}{2} \left[1 + \frac{12h}{W}\right]^{-1/2} \quad (2)$$

where h represents the substrate thickness. The patch length is determined by utilizing the following equation [22].

$$L = \frac{c}{2f_0\sqrt{\epsilon_{eff}}} \quad (3)$$

Due to fringing, the antenna's size is expanded electrically by a factor of ΔL . The longer length is provided by,

$$\Delta L = 0.412h \frac{(\epsilon_{eff} + 0.3)\left(\frac{W}{h} + 0.264\right)}{(\epsilon_{eff} - 0.258)\left(\frac{W}{h} + 0.8\right)} \quad (4)$$

Eqs. (5) and (6) are used to determine the substrate's minimal length (L_{sub}) and width (W_{sub}).

$$L_{sub} = 6h + L \quad (5)$$

$$W_{sub} = 6h + W \quad (6)$$

On the FR-4 dielectric substrate, an inset feed microstrip patch antenna employing copper is built using the above formulae [22]. The slotted rectangular shapes are etched on the patch after several optimizations. As the antenna is made for several observable frequencies, only its length and width must be altered; the basic structure is the same for all.

3.2 Proposed Antenna Design

A microstrip patch antenna is formed by etching out a metallic patch on a dielectric substrate material. On a ground plane, the dielectric material is mounted. A ground plane is a horizontal conducting surface that is flat or almost flat and used as part of an antenna in communications to reflect radio waves from other antenna elements.

Selecting the substrate is the priority in designing an antenna. The attributes of the substrate, such as the dielectric constant (ϵ_r), tangent loss ($\tan\delta$), and thickness (t_s) have an impact on the impedance matching and the bandwidth of an

antenna. A very thin substrate may result in high copper losses, but a thicker substrate may degrade the antenna's performance because of surface waves. Due to its low dielectric constant and loss dispersion, Roger RT5880 dielectric material is utilized as the substrate layer for developing the suggested antenna. It is a suitable material for UHF and SHF applications. Its electrical properties are presented in Table 2.

Table 2 Electrical Properties of Rogers RT5880 Dielectric Material

Name of the attributes	Values
Dielectric constant (ϵ_r)	2.2
Tangent loss ($\tan \delta$)	0.0009
Thermal cond.	0.2 [W/K/m]

One of the most widely used types of microstrip antennas is the rectangular patch antenna. Several strategies are utilized to improve the radiation properties of the patch antenna. Slot structure on the patch and defective ground structure (DGS) are the most frequently employed. For microstrip antennas, coaxial feed is among the most used feeding techniques.

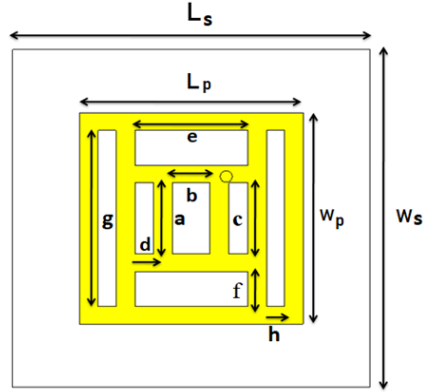
Fig. 3 depicts the geometrical structure of the proposed slotted patch antenna along with its complete ground plane. Using the CST-MWS Simulation Tool, the suggested design and simulation have been performed. Fig. 3(a) and (b) show the top and bottom layers of the antenna, respectively. It comprises a multiple-slotted square patch, Roger RT5880 dielectric substrate layer with a thickness of 1.575 mm, and a complete ground surface. As the ground plane and radiating patch, copper material with a thickness of 0.02 mm is utilized. The optimized dimension of the antenna is $38 \times 38 \times 1.575 \text{ mm}^3$. Many rectangular slots have been introduced into the square patch to improve the antenna's performance and shift the operating frequency into the desired Sub-6 GHz application band. The square-shaped radiating patch contains seven rectangular slots divided into four different types. The patch's dimensions ($L_p \times W_p$) is $23.76 \times 23.76 \text{ mm}^2$. Table 3 presents the parameters of the recommended patch antenna.

Table 3 Parameters of the recommended patch antenna

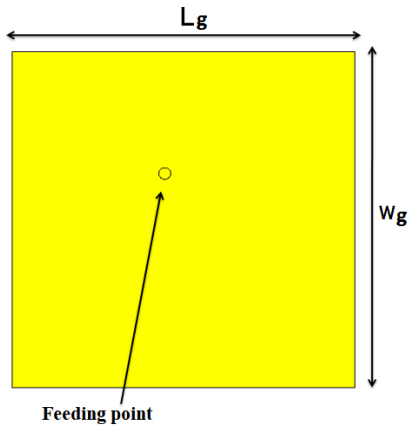
Parameters	Dimensions (mm)	Descriptions
L_s	38	The length of the substrate
W_s	38	The width of the substrate
L_g	38	The ground plane length
W_g	38	The ground plane width
t_s	1.575	The thickness of the substrate
t_g	0.02	Thickness of the copper ground plane
L_p	23.76	Square patch length
W_p	23.76	Square patch width
t_p	0.02	Thickness of the copper patch
x	3.71	Distance of feeding point from X-axis
y	4.7	Distance of feeding point from Y-axis

In Fig. 3(a), the central rectangular slot with dimensions ($a \times b$) of $8 \times 4 \text{ mm}^2$ is considered the first type-rectangular

slot. However, the second type-rectangular slots, are the two identically sized ($c \times d = 8 \times 1.9 \text{ mm}^2$) slots on both sides of the central slot. Additionally, the upper and lower sides of two rectangular slots from the first type-rectangular slot are the third type of rectangular slot and possess the same dimensions ($e \times f = 12 \times 3.9 \text{ mm}^2$). The two rectangular slots located on either side of the third type slot are the fourth type-rectangular slots that are similar in size.



(a) Top layer



(b) Bottom layer

Fig. 3 The geometrical structure of the recommended slotted patch antenna with the complete ground plane (without DGS) (a) Top layer (b) Bottom layer

Table 4 presents the dimension details of different rectangular slots. It is excited using a coaxial 50Ω probe feed. The feeding location of the coaxial probe is indicated by the little circle that is situated in the patch and ground plane. The feed is placed at 3.71 mm and 4.7 mm distances from the X and Y axes to ensure impedance matching, respectively.

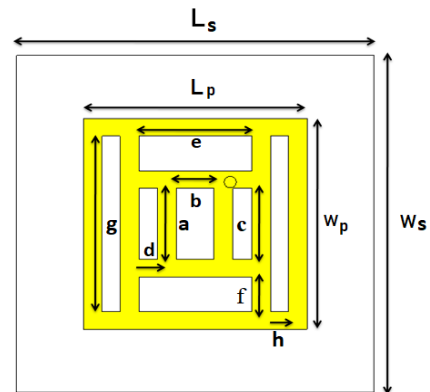
An emerging technique called defected ground structure (DGS) improves the narrow bandwidth, return loss, high selectivity, impedance profile, and other characteristics of antennas, filters, and other microwave components [20], [32]. With all the dimensions remaining the same, the suggested slotted patch antenna is then applied to the defected ground surface to improve the performance characteristics shown in Fig. 4. A rectangular slot with the dimension ($p \times q$) of $9 \times 7 \text{ mm}^2$ has been introduced into the copper ground plane. This rectangular shape of DGS has been used to disturb the electric field (E-field) on the ground surface. Table 5 depicts the dimensions of the ground plane's rectangular slot. The top and

bottom layers of the defective ground slotted patch antenna (DGSPA) are demonstrated in Fig. 4(a) and (b) respectively.

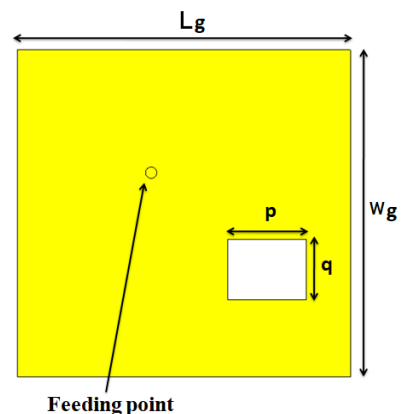
Table 4 Dimension details of different rectangular slots

Parameters	Dimensions (mm)	Descriptions
a	8	Length of the 1 st type of rectangular slot
b	4	Width of the 1 st type of rectangular slot
c	8	Length of the 2 nd type rectangular slot
d	1.9	Width of the 2 nd type rectangular slot
e	12	Length of the 3 rd type rectangular slot
f	3.9	Width of the 3 rd type rectangular slot
g	19.8	Length of the 4 th type rectangular slot
h	1.9	Width of the 4 th type rectangular slot

After slotting the ground surface, the performance characteristics of the proposed antenna are significantly changed. The performance of the antenna with DGS is significantly better than that of the antenna without DGS, which is elaborately discussed in the simulation result section. The comparative findings of the proposed antenna without DGS and with DGS are shown in Table 6.



(a) Top layer



(b) Bottom layer

Fig. 4 The geometrical structure of the recommended ground slotted patch antenna (with DGS) (a) Top Layer (b) Bottom Layer

Table 5 Dimensions of the ground plane’s rectangular slot

Parameter	Dimension (mm)	Description
p	9	Length of the rectangular slot in the ground plane
q	7	Width of the rectangular slot in the ground plane

4 Simulated Results and Performance Analysis

The recommended slotted 5G patch antenna had been designed and simulated using the 3D simulation software CST Microwave Studio 2017v. In this section, the performance parameters of the recommended antenna, such as reflection coefficient, radiation pattern, impedance profile, efficiency, E-field distribution, etc., are elaborately discussed based on the simulation results.

4.1 Reflection Coefficient, Bandwidth, and VSWR

The S-parameter’s ($S_{1,1}$) magnitude, measured in decibels (dB), represents the return loss. Fig. 5 depicts the return loss ($|S_{1,1}|$) graph for the suggested slotted 5G patch antenna in both the “without DGS” and “with DGS” cases. In the absence of DGS (without DGS), the antenna operates from 3.6106 GHz to 3.6682 GHz frequency, offering an impedance bandwidth of 57.6 MHz and resonating at 3.6396 GHz with a return loss of -37.916 dB. In the presence of DGS (with DGS), it operates from 3.4828 GHz to 3.552 GHz frequency and resonates at 3.5176 GHz with an excellent return loss of -54.028 dB. Therefore, the impedance bandwidth is increased by 11.6 MHz because of introducing DGS, and the return loss is decreased by -16.112 dB.

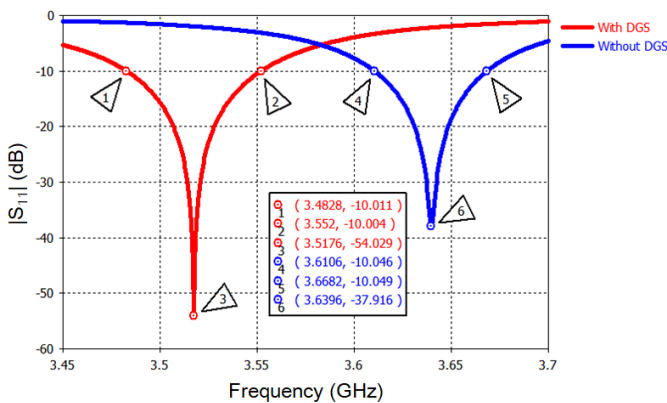


Fig. 5 The suggested slotted 5G patch antenna’s return loss ($|S_{1,1}|$) graph for both the “without DGS” and “with DGS” scenarios

Voltage standing wave ratio (VSWR) indicates how mismatched an antenna and its feeding component are. For antenna and RF applications, the value of VSWR should be less than 2. But unity (VSWR = 1) VSWR ensures the antenna’s impedance is properly matched. The VSWR of the suggested model for both cases is shown in Fig. 6. When DGS is absent, the antenna’s VSWR is 1.0276. When DGS is present, the antenna exhibits approximately unity VSWR ($1.004 \approx 1$), which

is an improvement above the value of VSWR when DGS is not present. Also, it ensures proper impedance matching for the antenna.

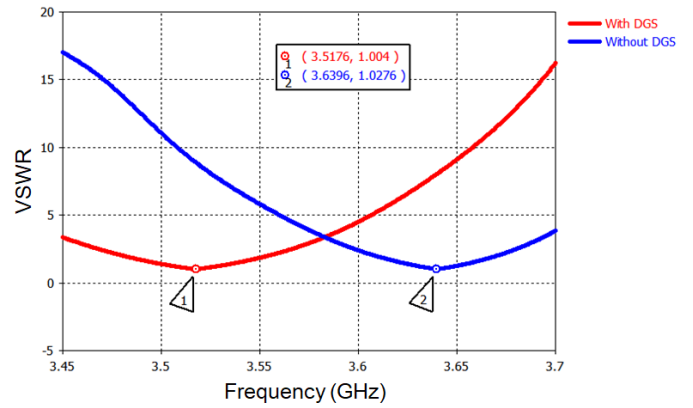
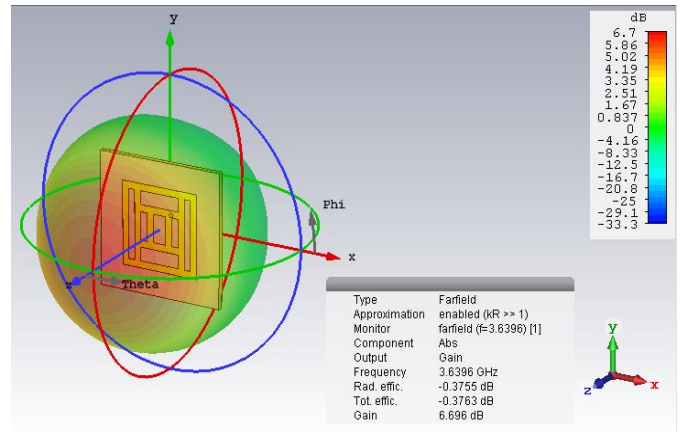


Fig. 6 The VSWR graph of the suggested slotted 5G patch antenna for both the “without DGS” and “with DGS” scenarios

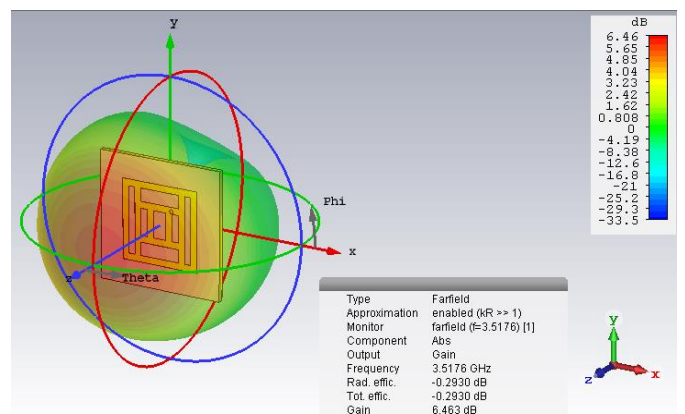
4.2 Radiation Pattern, Gain and Directivity

An antenna’s radiation pattern shows the mode of energy transmission or reception. On the other hand, the radiation gain of an antenna describes how well it converts the power input into radio waves and directs it in a specific direction or how well it converts radio waves from a certain direction into electrical energy.

Fig. 7 shows the simulated 3D gain of the recommended slotted patch antenna. The antenna exhibits a 3D radiation gain of 6.463 dB in the presence of DGS at the resonant frequency of 3.5176 GHz. On the other hand, the beam gain without the DGS structure of the antenna is depicted as 6.696 dB.



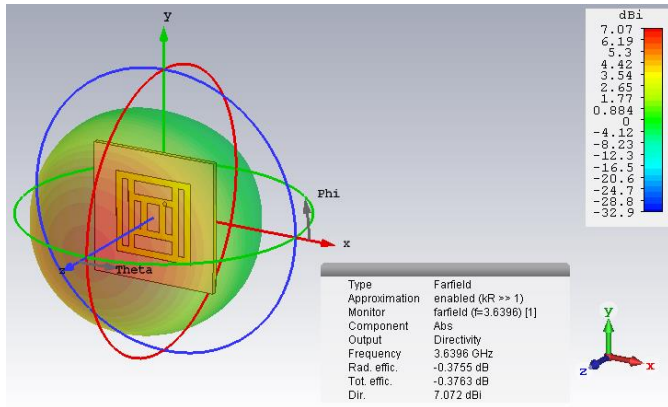
(a) Without DGS



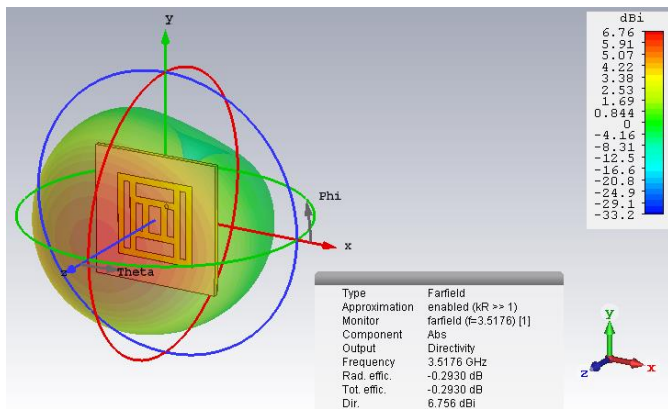
(a) With DGS

Fig. 7 3D radiation gains of the suggested slotted 5G patch antenna model (a) Without DGS (b) With DGS

Moreover, the antenna’s main lobe defines the direction of maximum radiation, known as directivity. As seen in Fig. 8, the 3D directivity by applying the DGS technique at the resonance frequency of 3.5176 GHz is 6.756 dBi. Without slotting the ground, its directivity is 7.072 dBi.



(a) Without DGS



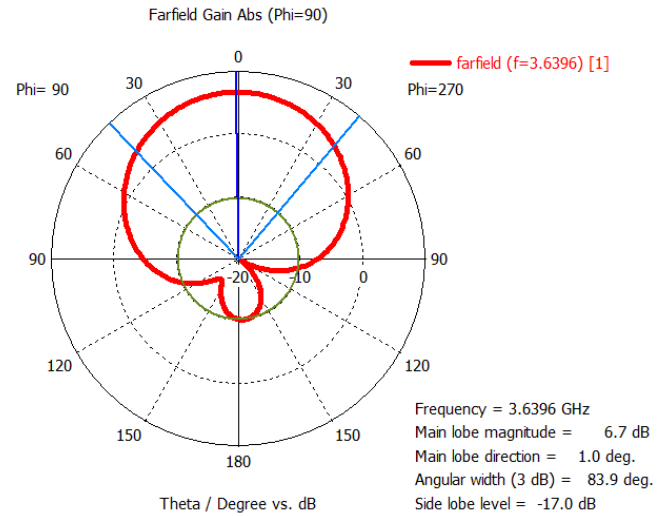
(b) With DGS

Fig. 8 3D directivity of the suggested slotted 5G patch antenna model (a) Without DGS (b) With DGS

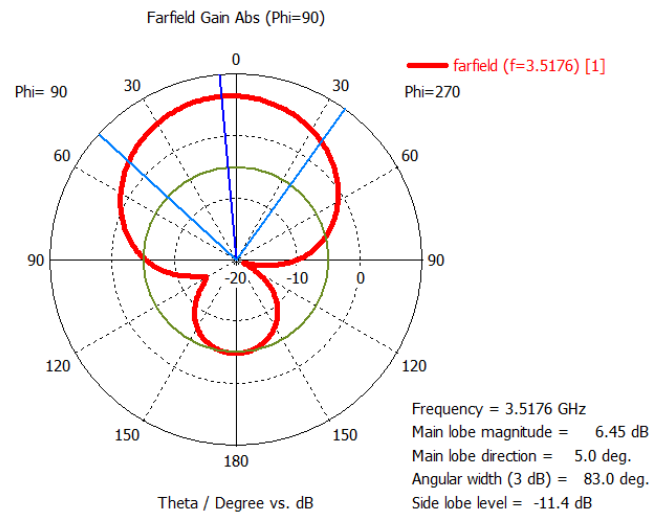
An antenna’s radiating farfield term is the region where the effective radiation pattern is observed. Fig. 9(a) and (b) demonstrate the polar radiation pattern (Farfield gain Abs) for both cases when $\phi = 90^\circ$. Without DGS, the major lobe’s magnitude, and angular width (3 dB) at 3.6396 GHz are 6.7 dB and 83.9°, respectively. As seen in Fig. 9(b), the main lobe’s magnitude and angular width (3 dB) at the resonance frequency of 3.5176 GHz are 6.45 dB and 83°, respectively, in the presence of DGS. In addition, its side lobe level is -11.4 dB.

Alternatively, when $\phi = 0^\circ$, the polar radiation pattern (Farfield Directivity Abs) for both cases is illustrated in Fig. 10(a) and (b). The main lobe has a magnitude level of 7.07 dBi and a direction of 0° in the absence of DGS, as shown in Fig. 10(a). Additionally, the angular width and side lobe level are 88.6° and -17 dB, respectively. Fig. 10(b) shows that the major lobe in the presence of DGS has a magnitude level of 6.71 dBi, and the angular width is 92°. Moreover, its direction is 3° , and the side lobe level is -11.3 dB. The directive pattern’s angular beam width at 3 dB is higher than the gain pattern, both with and

without slotting. On the other hand, the side lobe values for the gain and directive pattern are reversely equal before and after slotting.

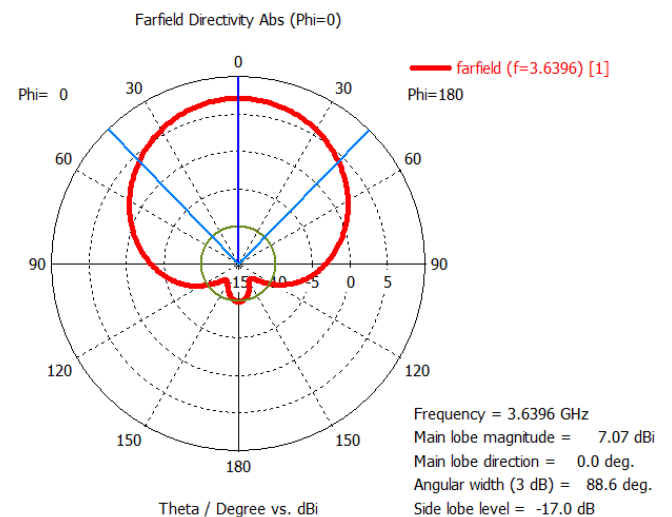


(a) Without DGS



(b) With DGS

Fig. 9 Farfield (2-D) gain pattern of the suggested slotted patch antenna when $\phi=90^\circ$ (a) Without DGS (b) With DGS



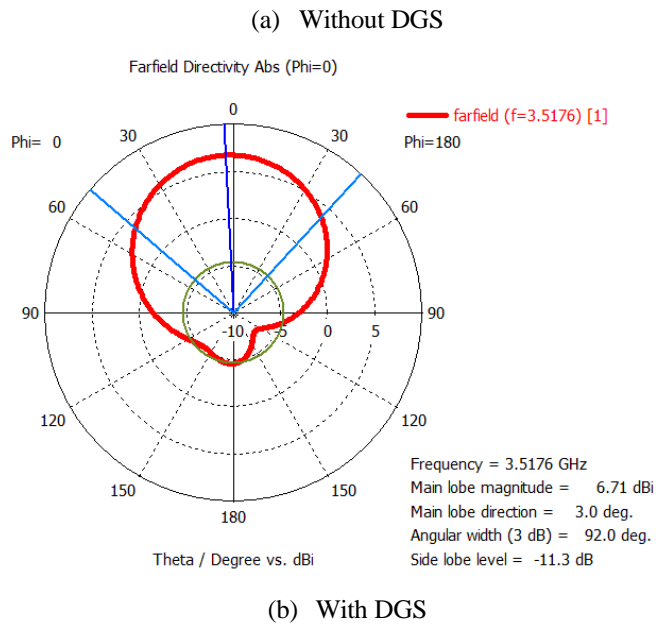


Fig. 10 Farfield (2-D) gain pattern of the suggested slotted patch antenna when $\phi=0^\circ$ (a) Without DGS (b) With DGS

The suggested antenna’s gain versus frequency 1-D linear graph is shown in Fig. 11 for both cases. Without slotting the ground plane, its gain is 6.6959 dB. Applying the DGS technique results in a gain of 6.4628 dB at a resonance frequency of 3.5176 GHz. Fig. 12 shows a 1D linear graph of the antenna’s directivity versus frequency. The antenna’s directivity is 6.7486 dBi and 7.0706 dBi, respectively, with and without DGS. As a result, after slotting the ground, the gain and directive values are reduced.

4.3 Impedance Profile, Efficiency, Surface Current, and E-field

The proposed defected ground slotted patch antenna (DGSPA), also known as the antenna with DGS, has an impedance profile (Z-Parameter) of $(50.086 - j0.179) \Omega$, which is shown in Fig. 13. It denotes 50Ω pure resistivity at the resonance frequency of 3.5176 GHz. Fig. 14 demonstrates the proposed antenna model’s radiation efficiency versus frequency graph. The antenna’s efficiency when DGS is not present is 91.718%. After using the DGS technique, the suggested antenna’s efficiency has increased; at the resonant frequency, the efficiency is approximately 93.475%.

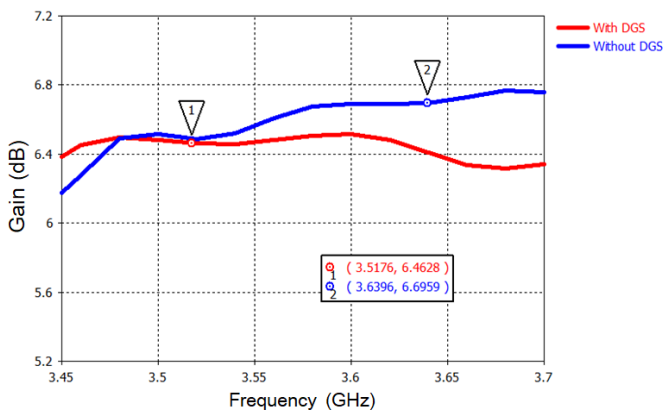


Fig. 11 Gain versus frequency 1-D linear graph for both the “without DGS” and “with DGS” scenarios of the proposed slotted 5G patch antenna

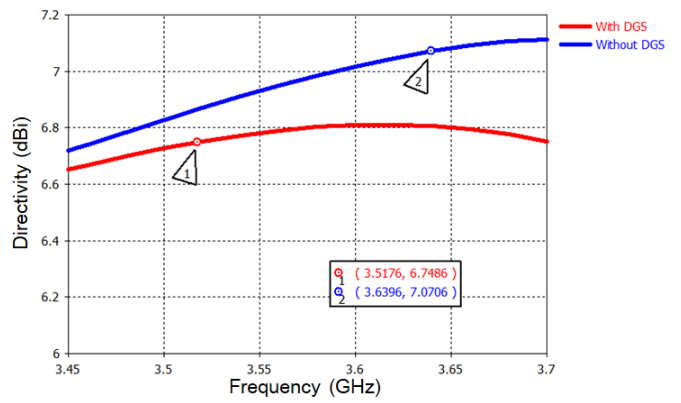


Fig. 12 Directivity versus frequency 1-D linear graph for both the “without DGS” and “with DGS” scenarios of the proposed slotted 5G patch antenna

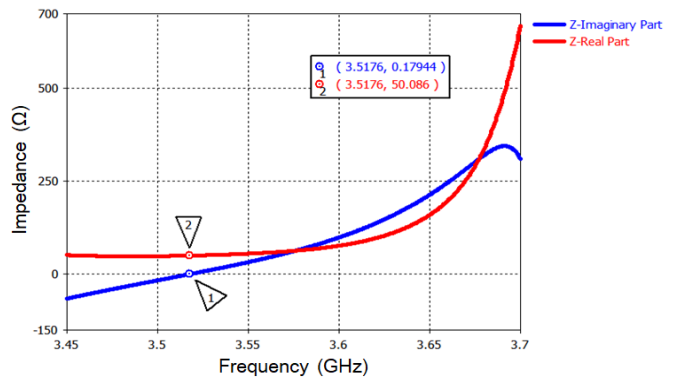


Fig. 13 Impedance profile of the proposed defected ground slotted patch antenna (DGSPA) at 3.5176 GHz resonant frequency

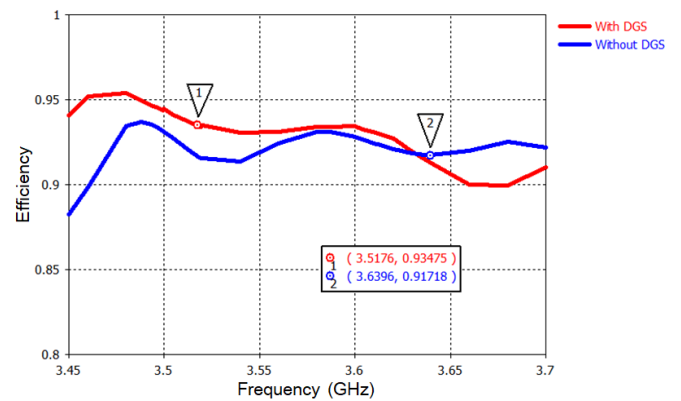


Fig. 14 Efficiency versus frequency graph for both the “without DGS” and “with DGS” scenarios of the suggested slotted patch antenna

The current distribution through the patch of the proposed 5G patch antenna at 3.5176 GHz (with DGS) and 3.6396 GHz (without DGS) frequency is depicted in Fig. 15. On the radiating patch, a strong surface current distribution is noticed around the rectangular slots that are mainly responsible for creating the 5G frequency band. Through the patch, the red color indicates the highest current density, while the blue hue indicates the lowest current density. It is seen that after slotting, the current density through the patch is increased. Fig. 15(a) shows a strong electric current through the patch at 3.5176 GHz frequency.

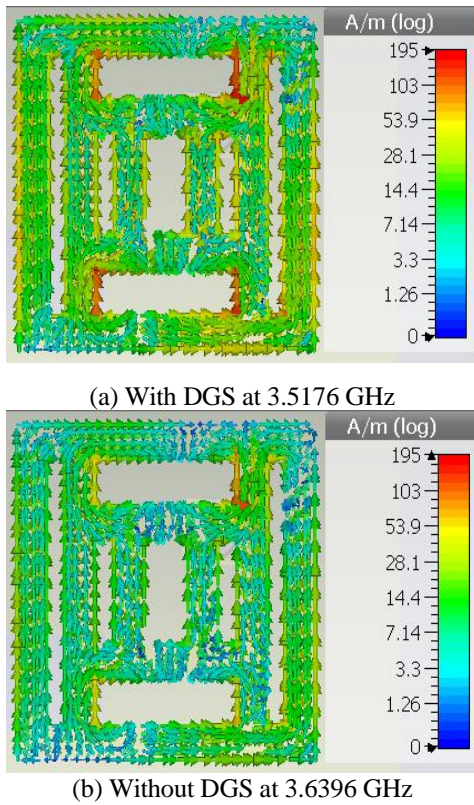


Fig. 15 Current distributions through the patch of the suggested 5G antenna (a) With DGS (b) Without DGS

The distributions of the E-field through the designed antenna at 3.5176 GHz (with DGS) and 3.6396 GHz (without DGS) frequency are shown in Fig. 16.

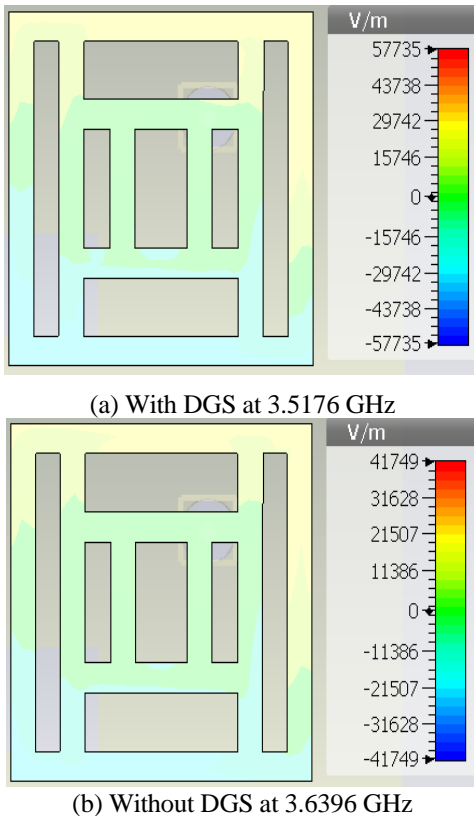


Fig. 16 Distributions of the E-field within the proposed patch antenna (a) With DGS (b) Without DGS

A strong distribution of the E-field is obtained at the 3.5176 GHz frequency band. An approximately 57735 V/m E-field present through the antenna patch at this frequency is illustrated in Fig. 16(a). During 3.6396 GHz frequency, an approximately 41749 V/m E-field exists at the antenna patch. Nevertheless, it has been seen that the E-field is focused within the patch and at the outer edges of the radiating patch. It forms the energy loop and enables effective radiation. Moreover, the E-field around the patch is very high after ground slots compared to the shape without slotting. The comparative study of the suggested slotted 5G patch antenna for both with and without DGS is presented in Table 6.

Table 6 The comparative findings of the proposed slotted patch antenna without DGS and with DGS

Proposed antenna	Without DGS	With DGS
Frequency (GHz)	3.6396	3.5176
Return loss (dB)	-37.916	-54.028
VSWR	1.0276	1.004
Bandwidth (MHz)	57.6	69.2
Gain (dB)	6.696	6.463
Efficiency	91.718%	93.475%

5 Comparison with Relevant Work

For use in 5G wireless applications, several types of antennas are presented in the literature [19]-[41], some of which are larger or have lower performance. Small antennas with improved performance are required for 5G communication technology. In Table 7, there is a comparison of the recommended defected ground slotted patch antenna (DGSPA) with the previously published works. In terms of the reflection coefficient ($|S_{1,1}|$), impedance bandwidth, radiation gain, impedance profile, radiation efficiency, etc., the recommended antenna model exhibits excellent performance.

Table 7 Comparison of the recommended defected ground slotted patch antenna (DGSPA) with several relevant previous works

Ref.	Antenna Size (mm ³)	Frequency (GHz)	BW (MHz)	Gain (dB)
[19]	34 × 18 × 1.6	3.5	100	2.6
[25]	100 × 100 × 1.6	3.5	23.6	7.55
[26]	45 × 40 × 4.5	3.5	196	6.391
[27]	50 × 30 × 1.575	3	50	7.52
		3.3	50	5
[28]	60 × 70 × 1.6	3.51	~100	6.77
[30]	47 × 31.69 × 1.575	3.50	129.7	4.660
[31]	52.92 × 55.56 × 1.2	5.65	135	7.15
[32]	47.46 × 36.57 × 1.5	3.5305	116.4	N/A
[41]	32.4 × 27.9 × 1.6	3.5	19	4.2
This Work	38 × 38 × 1.575	3.5176	69.2	6.46

6 Conclusions

In this article, a coaxial-fed defected ground slotted patch antenna (DGSPA) is suggested for Sub-6 GHz 5G services. The proposed antenna's dimension is $38 \times 38 \text{ mm}^2$ with a thickness of 1.575 mm, and Rogers RT5880 material is utilized as the substrate layer to construct it. It can operate in the LTE Band 42, WiMAX, and the 5G N77 band. The special features of the recommended antenna are its compact size, proper impedance matching, improved impedance bandwidth, high efficiency, and high gain of the antenna. The antenna without DGS resonates at 3.6396 GHz with a return loss ($|S_{1,1}|$) of -37.916 dB, offering a bandwidth of 57.6 MHz. The operational frequency range of the antenna with DGS is from 3.4828 GHz to 3.552 GHz and has an excellent return loss of -54.028 dB at 3.5176 GHz resonance frequency and approximately unity ($1.004 \approx 1$) VSWR. Because of introducing DGS, 11.6 MHz increases the impedance bandwidth, and the return loss is decreased by -16.112 dB. Also, the DGS-backed antenna has an excellent impedance profile of $(50.086 - j0.179) \Omega$, which denotes 50Ω pure resistivity. Additionally, it exhibits a radiation gain of 6.463 dB and a radiation efficiency of 93.475% at the resonance frequency point. The suggested antenna would be a good option for use in 5G services due to its small size and excellent performance features.

References

- [1] AIRikabi, H.T.S., Alaidi, A.H., Abdalrada, A.S. and Abed, F.T., 2019. Analysis the Efficient Energy Prediction for 5G Wireless Communication Technologies. *Int. J. Emerg. Technol. Learn.*, 14(8), pp.23-37.
- [2] Habibi, M.A., Nasimi, M., Han, B. and Schotten, H.D., 2019. A comprehensive survey of RAN architectures toward 5G mobile communication system. *Ieee Access*, 7, pp.70371-70421.
- [3] Ullah, R., Ullah, S., Ullah, R., Faisal, F., Mabrouk, I.B. and Al Hasan, M.J., 2020. A 10-ports MIMO antenna system for 5G smart-phone applications. *IEEE access*, 8, pp.218477-218488.
- [4] Talukder, A. and Islam, E., 2021, December. Design and simulation study of e shaped slotted microstrip patch antenna by HFSS for 5G applications. In *2021 IEEE International Symposium on Antennas and Propagation and USNC-URSI Radio Science Meeting (APS/URSI)* (pp. 1909-1910). IEEE.
- [5] Attaran, M., 2023. The impact of 5G on the evolution of intelligent automation and industry digitization. *Journal of ambient intelligence and humanized computing*, 14(5), pp.5977-5993.
- [6] Attaran, M. and Attaran, S., 2020. Digital transformation and economic contributions of 5G networks. *International Journal of Enterprise Information Systems (IJEIS)*, 16(4), pp.58-79.
- [7] Biddut, N.H., Haque, M.E. and Jahan, N., 2022, March. A wide band microstrip patch antenna design using multiple slots at v-band. In *2022 International Mobile and Embedded Technology Conference (MECON)* (pp. 113-116). IEEE.
- [8] Rahman, M.M. and Ryu, H.G., 2021, October. Compact multiple wideband slotted circular patch antenna for satellite and millimeter-wave communications. In *2021 International Conference on Information and Communication Technology Convergence (ICTC)* (pp. 233-236). IEEE.
- [9] Nahas, M., 2022. Design of a high-gain dual-band LI-slotted microstrip patch antenna for 5G mobile communication systems. *Journal of Radiation Research and Applied Sciences*, 15(4), p.100483.
- [10] Saif, H.M., Abdo, E.A., Qahtan, A.H. and Shaddad, R.Q., 2021, August. Improved Performance in Compact Antenna by Using E-slotted and DGS for V and E band 5G Applications. In *2021 1st International Conference on Emerging Smart Technologies and Applications (eSmarTA)* (pp. 1-4). IEEE.
- [11] Moussa, F.Z., Ferouani, S., Belhadeif, Y. and Abdellaoui, G., 2021, December. New design of miniature rectangular patch antenna with DGS for 5G mobile communications. In *2021 International Conference on Information Systems and Advanced Technologies (ICISAT)* (pp. 1-5). IEEE.
- [12] Hasan, M.M., Islam, M.T., Samsuzzaman, M., Baharuddin, M.H., Soliman, M.S., Alzamil, A., Abu Sulayman, I.I. and Islam, M.S., 2022. Gain and isolation enhancement of a wideband MIMO antenna using metasurface for 5G sub-6 GHz communication systems. *Scientific reports*, 12(1), p.9433.
- [13] Prasad, B.S.H. and Prasad, M.V., 2020. Design and analysis of compact periodic slot multiband antenna with defected ground structure for wireless applications. *Progress In Electromagnetics Research M*, 93, pp.77-87.
- [14] Khandelwal, M.K., Kanaujia, B.K. and Kumar, S., 2017. Defected ground structure: fundamentals, analysis, and applications in modern wireless trends. *International Journal of Antennas and Propagation*, 2017.
- [15] Gopi, D., Vadaboyina, A.R. and Dabbakuti, J.K., 2021. DGS based monopole circular-shaped patch antenna for UWB applications. *SN Applied Sciences*, 3(2), p.198.
- [16] Nahas, M., 2022. A super high gain l-slotted microstrip patch antenna for 5G mobile systems operating at 26 and 28 GHz. *Engineering, Technology & Applied Science Research*, 12(1), pp.8053-8057.
- [17] Hmamouche, Y., Benjillali, M. and Saoudi, S., 2018, November. Closed-form Coverage Probability under the Idle Mode Capability: A Stochastic Geometry Approach. In *2018 9th International Symposium on Signal, Image, Video and Communications (ISIVC)* (pp. 135-140). IEEE.
- [18] Irfansyah, A., Harianto, B.B. and Pambudiyatno, N., 2021, November. Design of rectangular microstrip antenna 1x2 array for 5G communication. In *Journal of Physics: Conference Series* (Vol. 2117, No. 1, p. 012028). IOP Publishing.
- [19] Karimbu Vallappil, A., Khawaja, B.A., Rahim, M.K.A., Iqbal, M.N. and Chattha, H.T., 2022. Metamaterial-inspired electrically compact triangular antennas loaded with CSRR and 3×3 cross-slots for 5G indoor distributed antenna systems. *Micromachines*, 13(2), p.198.
- [20] Astuti, D.W., Fadilah, R., Muslim, D.R., Rusdiyanto, D., Alam, S. and Wahyu, Y., 2022. Bandwidth Enhancement of Bow-tie Microstrip Patch Antenna Using Defected Ground Structure for 5G. *J. Commun.*, 17(12), pp.995-1002.

- [21] Fadhil, T.Z., Murad, N.A., Rahim, M.K.A., Hamid, M.R. and Nur, L.O., 2021. A beam-split metasurface antenna for 5G applications. *IEEE Access*, 10, pp.1162-1174.
- [22] Noor, S.K., Jusoh, M., Sabapathy, T., Rambe, A.H., Vettikalladi, H., M. Albishi, A. and Himdi, M., 2023. A Patch Antenna with Enhanced Gain and Bandwidth for Sub-6 GHz and Sub-7 GHz 5G Wireless Applications. *Electronics*, 12(12), p.2555.
- [23] Hashim, F.F., Mahadi, W.N.L.B.W., Abdul Latef, T.B. and Othman, M.B., 2023. Fabric–Metal Barrier for Low Specific Absorption Rate and Wide-Band Felt Substrate Antenna for Medical and 5G Applications. *Electronics*, 12(12), p.2754.
- [24] Moussa, F.Z., Ferouani, S. and Belhadef, Y., 2022. New Design of Metamaterial Miniature Patch Antenna with DGS for 5G Mobile Communications. *Microwave Review*, 28(2).
- [25] Rana, M.S., Islam, S.I., Al Mamun, S., Mondal, L.K., Ahmed, M.T. and Rahman, M.M., 2022. An S-Band Microstrip Patch Antenna Design and Simulation for Wireless Communication Systems. *Indonesian Journal of Electrical Engineering and Informatics (IJEI)*, 10(4), pp.945-954.
- [26] Rahmawati, Y.N. and Ludiyati, H., 2021, November. The characteristic of a 3.5 GHz circular patch antenna using open-ring artificial dielectric. In *2nd International Seminar of Science and Applied Technology (ISSAT 2021)* (pp. 387-393). Atlantis Press.
- [27] Amjad, Q., Kamran, A., Tariq, F. and Karim, R., 2019, November. Design and characterization of a slot based patch antenna for Sub-6 GHz 5G applications. In *2019 Second International Conference on Latest trends in Electrical Engineering and Computing Technologies (INTELLECT)* (pp. 1-6). IEEE.
- [28] Song, R., Huang, G.L., Liu, C., Zhang, N., Zhang, J., Liu, C., Wu, Z.P. and He, D., 2019. High-conductive graphene film based antenna array for 5G mobile communications. *International Journal of RF and Microwave Computer-Aided Engineering*, 29(6), p.e21692.
- [29] Chen, W.S. and Lin, Y.C., 2018, August. Design of 2×2 Microstrip Patch Array Antenna for 5G C-Band Access Point Applications. In *2018 IEEE International Workshop on Electromagnetics: Applications and Student Innovation Competition (iWEM)* (pp. 1-2). IEEE.
- [30] Ramli, N., Noor, S.K., Khalifa, T. and Abd Rahman, N.H., 2020. Design and performance analysis of different dielectric substrate based microstrip patch antenna for 5G applications. *International Journal of Advanced Computer Science and Applications*, 11(8).
- [31] Tütüncü, B. and Kösem, M., 2022. Substrate analysis on the design of wide-band antenna for sub-6 GHz 5G communication. *Wireless Personal Communications*, 125(2), pp.1523-1535.
- [32] Hakanoglu, B.G., Sen, O., Koc, B., Hayber, S.E. and Turkmen, M., 2020, August. Defected Grounded Rectangular Patch Antenna with Rhombic-Shaped Slots for Early Phase 5G Applications. In *2020 XXXIIIrd General Assembly and Scientific Symposium of the International Union of Radio Science* (pp. 1-4). IEEE.
- [33] Ashfaq, M., Bashir, S., Shah, S.I.H., Abbasi, N.A., Rmili, H. and Khan, M.A., 2022. 5G antenna gain enhancement using a novel metasurface. *Computers, Materials & Continua*, 72(2), pp.3601-3611.
- [34] Awan, W.A., Hussain, N., Ghaffar, A., Zaidi, A. and Li, X.J., 2020, February. A compact flexible antennas for ISM and 5G sub-6-GHz band Application. In *WSA 2020; 24th International ITG Workshop on Smart Antennas* (pp. 1-3). VDE.
- [35] Rizvi, S.N.R., Mazher, A., Chaudary, E., Alibakhshikenari, M., Falcone, F. and Limiti, E., 2021, August. Wideband Small Fractal Antenna with Simple Design Strategy for 5G Sub-6-GHz Wireless Communications. In *2021 XXXIVth General Assembly and Scientific Symposium of the International Union of Radio Science (URSI GASS)* (pp. 1-4). IEEE.
- [36] Sree, M.F.A., Abd Elazeem, M.H. and Swelam, W., 2021, December. Dual Band Patch Antenna Based on Letter Slotted DGS for 5G Sub-6GHz Application. In *Journal of Physics: Conference Series* (Vol. 2128, No. 1, p. 012008). IOP Publishing.
- [37] Alwareth, H., Ibrahim, I.M., Zakaria, Z., Al-Gburi, A.J.A., Ahmed, S. and Nasser, Z.A., 2022. A wideband high-gain microstrip array antenna integrated with frequency-selective surface for Sub-6 GHz 5G applications. *Micromachines*, 13(8), p.1215.
- [38] Azim, R., Meaze, A.M.H., Affandi, A., Alam, M.M., Aktar, R., Mia, M.S., Alam, T., Samsuzzaman, M. and Islam, M.T., 2021. A multi-slotted antenna for LTE/5G Sub-6 GHz wireless communication applications. *International Journal of Microwave and Wireless Technologies*, 13(5), pp.486-496.
- [39] Khalilabadi, A.J. and Zadehgo, A., 2018, March. Multiband antenna for wireless applications including GSM/UMTS/LTE and 5G bands. In *2018 International Applied Computational Electromagnetics Society Symposium (ACES)* (pp. 1-2). IEEE.
- [40] Hussain, R., 2021. Shared-aperture slot-based sub-6-GHz and mm-wave IoT antenna for 5G applications. *IEEE Internet of Things Journal*, 8(13), pp.10807-10814.
- [41] Chowdhury, M.Z.B., Islam, M.T., Rmili, H., Hossain, I., Mahmud, M.Z. and Samsuzzaman, M., 2022. A low-profile rectangular slot antenna for sub-6 GHz 5G wireless applications. *International Journal of Communication Systems*, 35(17), p.e5321.
- [42] Balanis, C.A., 2016. *Antenna theory: analysis and design*. John Wiley & sons.